



Local Corrosion of the Oxide Passivation Layer during Cu Chemical Mechanical Polishing

Min Cheol Kang,^a Yung Jun Kim,^{*} Hyo-Chol Koo, Sung Ki Cho,^{*} and Jae Jeong Kim^{**z}

School of Chemical and Biological Engineering, Seoul National University, Seoul 151-742, Korea

In this article, we analyze the effect of complexing agents in Cu chemical mechanical polishing slurry on the formation of oxide and the evolution of stress. The passivation property and surface morphology of the oxide on the surface showed significant differences depending on the kind of complexing agent. Oxalic acid showed fast oxide formation with poor passivation performance, and this caused large tensile stress evolution over 250 MPa in the Cu film. The synergistic effect of stress evolution and temperature increase due to the friction during the polishing caused severe pitting of the Cu surface after polishing in oxalic-acid-based slurry.

© 2009 The Electrochemical Society. [DOI: 10.1149/1.3236391] All rights reserved.

Manuscript submitted June 16, 2009; revised manuscript received August 27, 2009. Published October 1, 2009.

The role of interconnections is to provide electrical connections to devices such as transistors so that signals can pass among them. The original tungsten and aluminum interconnection materials have been replaced with copper (Cu) because of its lower electrical resistance and higher electromigration resistance.¹⁻³ The Cu interconnections in current semiconductor manufacturing are fabricated through a damascene process using bottom-up filling of patterns by electrodeposition and chemical mechanical polishing (CMP), which removes overdeposited Cu. A more detailed understanding of the interaction between the slurry and the surface is increasingly important with the pattern density increases under delicate polishing conditions, such as fast polishing for more economical processing, with better uniformity on larger wafer surfaces, smoother surface morphology after polishing, minimum erosion or dishing damage regardless of the geometry, and control of the removal rate according to the materials.⁴⁻⁶ Corrosion of the surface by the slurry that causes dishing or surface roughening and galvanic corrosion after the second polishing step has been the focus of recent CMP research.⁷⁻¹¹

Copper CMP slurry generally contains an oxidizing agent, a complexing agent, inhibitors, and a pH buffering agent. Theoretical studies of the reaction mechanisms suggest that the complexing agent in Cu CMP usually accelerates Cu oxide dissolution, which enhances the polishing rate of Cu oxide.^{12,13} The role of the complexing agent in the CMP process, which usually has carboxylic acid or an amine group in its molecular structure, has been the subject of much research.¹⁴⁻¹⁸ These chemicals have different chemical reaction pathways for Cu in various environments even though they have similar functional groups.¹⁴⁻¹⁸ The differences could induce different polishing rates according to the slurry pH, oxide formation character differences, and deviations in the radical formation rate.¹⁹ However, there has been little research into the correlation between the difference in oxide formation and the corrosion character of various slurries. In this research, the stress evolution due to the oxide formation by the slurry and its effect on the corrosion pit generation was intensively studied. Furthermore, the effect of temperature increase during the friction pad polishing step and pit generation was also analyzed.

Experimental

In this research, a Cu wafer with a structure of Cu [9000 Å, physical vapor deposition (PVD)]/Ta (500 Å, PVD)/TaN (300 Å, PVD)/SiO₂ (10,000 Å, thermal oxidation)/Si(100) (4 in. wafer) was used for all the experiments. The electrochemical analyses were

conducted using a conventional three-electrode electrochemical cell with a potentiostat (model 263 A, EG&G). A Cu coupon wafer with a surface area of 1 cm² was used as the working electrode, and a Pt wire and a saturated calomel electrode were used as the counter and reference electrodes, respectively. The anodic current was measured at the corrosion potential in various slurry solutions without alumina powder determined from a Tafel plot.

The Cu wafer was polished using the R&D POLI-400 CMP machine (G&P Tech., Korea) to evaluate pit generation after CMP. The polishing pad was a 16 in. IC 1000/SUBA 4 pad supplied by Rodel Inc. The platen speed was 80 rpm and the carrier speed was 75 rpm. The pressure applied between the platen and the carrier was maintained at 2.5 psi, and the flow rate of the slurry was set to 150 mL/min. The substrate used in the polishing test for observing pits was a trench-type patterned wafer, where the trench depth was 500 nm, with Cu (3000 Å, PVD)/Ta (500 Å, PVD)/TaN (300 Å, PVD)/SiO₂ (10,000 Å, thermal oxidation)/Si. The temperature of the slurry was measured by IR thermometer (910.0500/IRVL LAB from Alle France, ±2°C accuracy) after the end of polishing and lift-up of the wafer from the pad. It was assumed that the slurry was in thermal equilibrium with the pad as well as the wafer during their physical contact. The data were obtained from a single-run experiment, and the local deviation of the temperature was measured.

The stress evolution during the oxide formation caused by dipping the Cu wafer into various slurry solutions was measured using a thin-film stress measurement device (FLX-2320, KLA-Tencor, less than ±2.5% or 1 MPa accuracy) to determine the change in the wafer curvature. To prevent recrystallization of the dipped wafers, they were kept in dry ice until the stress measurement took place. X-ray diffraction (XRD), atomic force microscopy (AFM), and field-emission scanning electron microscopy (FESEM) were also used to characterize the film properties after dipping.

The composition of the slurry for CMP consisted of 2.5 wt % Al₂O₃ as an abrasive, 2 wt % H₂O₂ as an oxidizing agent, with and without 0.02 M oxalic acid or citric acid used as a complexing agent. The slurry pH was fixed at 4.0 using H₂SO₄ or KOH solution. The wafer was dipped into the slurry for 10 min and rinsed in deionized water to remove the remaining slurry. After these processes, the water droplets were removed with a N₂ blow gun. The changes in sheet resistances were used to calculate the static etch rate of the Cu wafer using the following equation

$$\Delta t = \rho \left(\frac{1}{R_{s1}} - \frac{1}{R_{s2}} \right)$$

Results and Discussion

Figure 1 shows the change in the anodic current as a function of the immersion time of the Cu wafer in various slurry solutions. In H₂O₂ and oxalic acid solution, the anodic current decreased due to the reduction in the active area where the oxidation reaction of Cu

* Electrochemical Society Student Member.

** Electrochemical Society Active Member.

^a Present address: Hynix Semiconductor Inc., Advanced Process Research and Development Division, Icheon 467-701, Korea.

^z E-mail: jikimm@snu.ac.kr

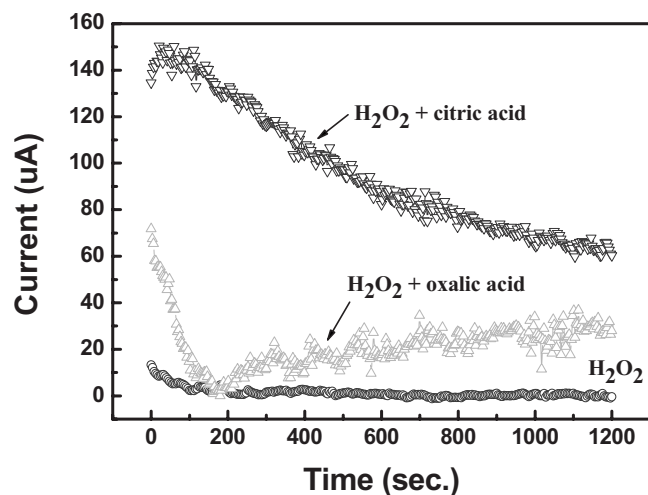


Figure 1. Changes in anodic currents at the corrosion potential on Cu dipped in slurry solutions.

occurred due to the formation of Cu oxide that blocked available reaction sites. With oxalic acid, the amount of charge was larger than in H_2O_2 alone. Furthermore, the anodic current gradually increased after 180 s although the Cu surface was passivated by the Cu oxide in the oxalic-acid-based solution. These results suggested that the oxide formed during the early stage of the dissolution was quite porous, so continuous dissolution could occur. The current density was larger than in the case without oxalic acid, and the exposed area was continuously reduced, as indicated by the sharp decrease in current density until 180 s. After 180 s, some part of the oxide was damaged, and the Cu film was again exposed to the slurry, which induced reoxidation or redissolution of the Cu. When the Cu wafer was immersed into a citric-acid-based solution, there was no sharp decrease in the anodic current, which implies that there was no passivation oxide layer formed. Some research into citric-acid-based solutions suggests that the dissolution of Cu oxide by complexing with citrate is quite fast.¹⁸ Therefore, the passivation character of the H_2O_2 alone or H_2O_2 with oxalic acid or citric acid showed significant differences in the oxide formation and passivation performance.

The surface morphology of the Cu after dipping in various slurry solutions was examined through FESEM and AFM phase image analysis (Fig. 2). For oxalic acid, the Cu surface was covered with less-dense Cu oxide compared to that obtained with the H_2O_2 -only solution. A phase image revealed the difference in the materials by the different friction coefficient of the surface, and the images indicated that two types of materials coexisted on the surface, possibly Cu and Cu oxide. Therefore, we confirmed that the increase in anodic current was caused by the partial exposure of the Cu surface in the slurry.

The generated stress was measured by the change in the curvature of the new Cu wafer before and after immersion in a H_2O_2 solution, with and without a complexing agent for 2 min; Fig. 3 shows the result. When a Cu wafer was immersed in an oxalic-acid-based solution, the largest stress (tensile, 281 MPa average) occurred. The value of the generated stress also gradually decreased as the measurement proceeded. The measured stresses were 165 and 114 MPa in H_2O_2 - and citric-acid-based solutions, respectively. The stress evolution was due to the volume expansion of the Cu oxide compared to its original nature, and the total amount of the oxide formation was related to the measured stress value. The highest OH radicals in previous research compared to the H_2O_2 solution were produced when oxalic acid was added to a H_2O_2 solution. Oxalic acid produced a thicker oxide film than the citric-acid-based solution or H_2O_2 -only solution.¹⁹ The stress determined by the measurement of the wafer curvature is biaxial stress, which is intrinsically gener-

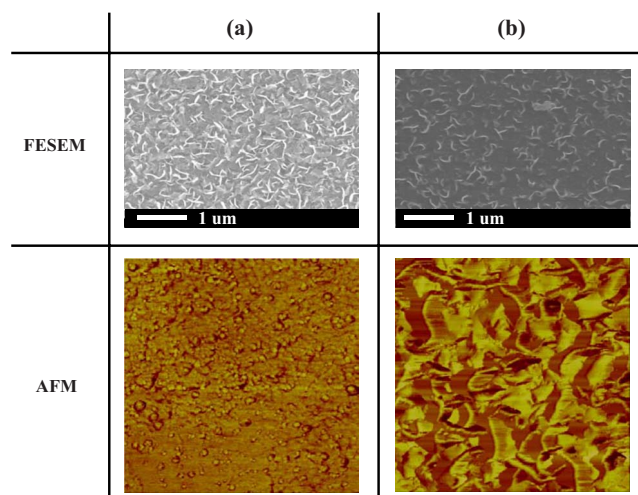


Figure 2. (Color online) FESEM and AFM phase images of Cu after immersing in (a) 2 wt % H_2O_2 -only solution and (b) 0.02 M oxalic acid and 2 wt % H_2O_2 solutions for 10 min. The scan size of AFM images was 1 μm^2 .

ated from the chemical modification. During the polishing process, the pressure to push the wafer to the pad was applied normal to the surface. The value is approximately 17 MPa and was uniformly applied to the surface. Other stress, caused by the friction with the pad, would also evolve. This is thought to have an insignificant effect on the chemical reaction of the surface, as the friction force removes the oxide films and would prevent the accumulation of the stress.

A strong evolution of Cu (200) texture was also observed after dipping samples in oxalic-acid-based solution. As shown in Fig. 4, when the Cu wafer was dipped into the H_2O_2 or citric-acid-based solution, the texture of Cu(111) predominated, and the ratios of Cu(111):(200) were 23 and 25, respectively. After the wafer was dipped into the oxalic acid slurry, the texture of Cu (200) was enhanced and the ratio of Cu(111):(200) decreased dramatically to 2. When a large stress over a certain critical value was applied to the Cu film to relax the stress, (200) texture evolution was observed.²⁰ There might be some relationship between this increase in (200) texture and stress decrease during the measurement time in the sample dipped in the oxalic-acid-based solution. Furthermore, the enhanced (200) texture due to stress evolution could also accelerate the formation of cracks or pits and chemical dissolution at the oxide

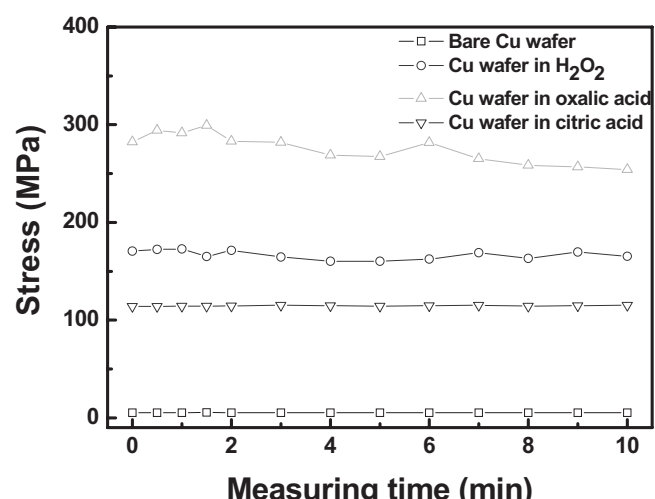


Figure 3. Stresses of the Cu wafer dipped in various solutions for 2 min.

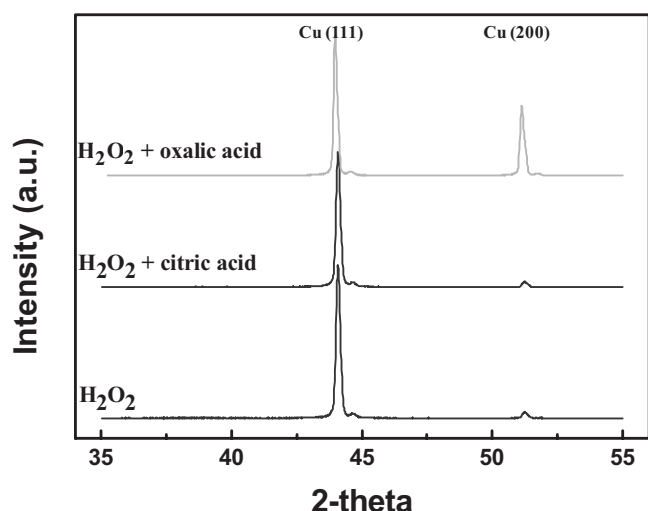


Figure 4. XRD spectra of the Cu wafer after immersing for 2 min in 2 wt % H₂O₂ solution with and without 0.02 M oxalic acid or citric acid.

or Cu layer.²¹ The texture modification due to stress and enhanced corrosion or pit generation due to the texture modification would have a synergistic effect on the continuous oxidation in the oxalic-acid-based solution.

The temperature of the slurry and the pad increased during CMP because of the friction between the wafer and the pad. The etch and removal rates are strongly affected by the increase in slurry temperature.^{22,23} Figure 5 shows the change in slurry temperature for various solutions measured with an IR thermometer during CMP. The slurry exhibited a 9–13°C increase in temperature in 120 s. The highest slurry temperature of 33°C was obtained when using H₂O₂ slurry. Because the slurry temperature was measured after detaching the wafer from the pad, the actual temperature of the slurry during the polishing step was slightly higher than that measured. Figure 6 shows that the etch rate of Cu increased linearly as the temperature of the solution increased. This result also suggests that the measurement of the etch rate at room temperature could be seriously distorted by the temperature effect.

Figure 7 shows the surface morphology of the polished Cu in the recess area using H₂O₂ slurry with oxalic acid or citric acid. Many pits were observed on the polished Cu when using the oxalic-acid-

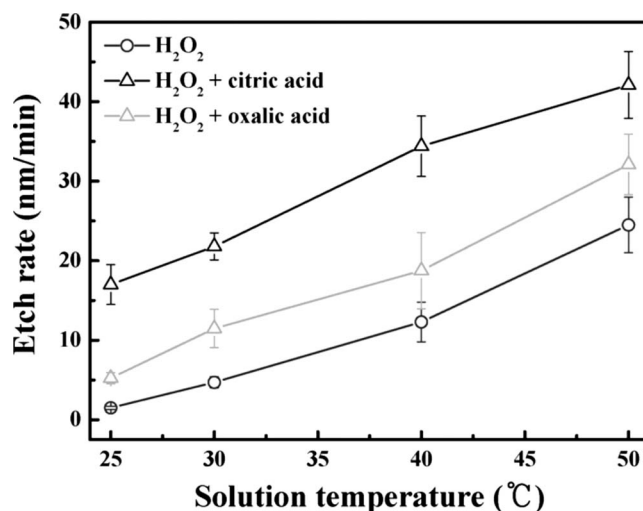


Figure 6. Etch rates of Cu in 2 wt % H₂O₂ solution and 2.5 wt % alumina particles with and without 0.02 M oxalic acid or citric acid with various solution temperatures.

based slurry. The major reaction was the etch process by the slurry in the recess area where the pressure of the pad was weaker than the dielectric surface. Because the Cu thickness in the trench was lower than the pattern depth in this study, only the Cu surface had contact with the slurry. Therefore, this implies that the synergistic actions of stress generation and increase in slurry temperature led to the formation of pits through local corrosion.

Conclusion

The effects of stress and slurry temperature on corrosion during Cu CMP were investigated. The anodic current measurement showed that the oxalic acid had a passivation–oxidation reaction, the citric acid solution showed no passivation effect, and the H₂O₂-only solution showed good passivation due to dense oxide film formation. The results of the stress measurement indicates that the Cu film faces a large tensile stress that might be caused by the formation of Cu oxide. The generated stress was the highest when oxalic acid was added, resulting in the breakdown of Cu oxide by the crack or pit formation and the exposure of new Cu surfaces in the solution, followed by continuous oxidation or dissolution. There was a linear relationship between the slurry temperature and the etch rate regardless of the slurry composition. These two results, the stress evolution and temperature increase by friction, in particular, could have a syn-

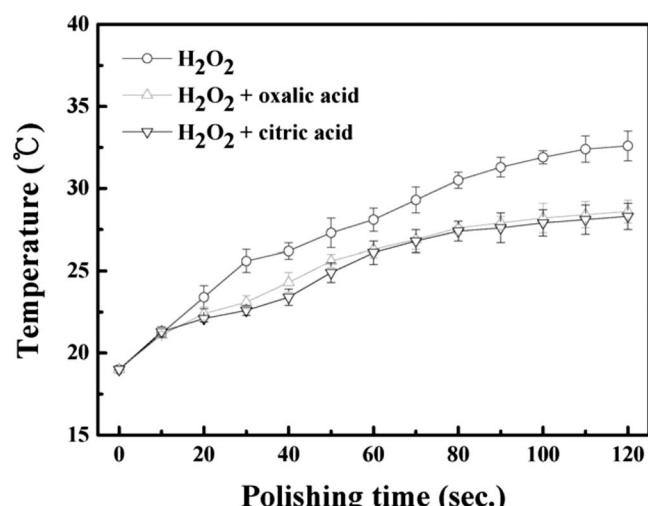


Figure 5. Temperature variation in various slurries according to polishing process time measured by an IR thermometer.

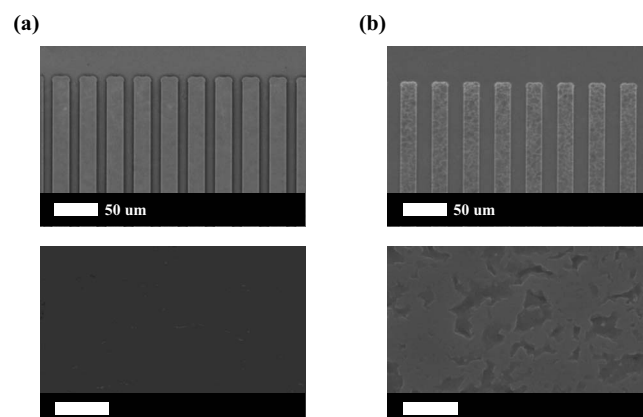


Figure 7. FESEM images of the polished Cu pattern structure (first row) and the magnified Cu surface (second row) using (a) citric-acid- and (b) oxalic-acid-based slurries.

ergistic effect on the damage formation of the Cu surface. Therefore, an accurate understanding of the effect of complexing agents and temperature control must be considered in the decision on slurry composition.

Acknowledgments

This work was supported by the Korea Science and Engineering Foundation through the Research Center for Energy Conversion and Storage, the Fundamental Research and Development Program for Core Technology of Materials funded by the Korean Ministry of Commerce, Industry, and Energy, and by the Institute of Chemical Processes at Seoul National University.

Seoul National University assisted in meeting the publication costs of this article.

References

1. S. P. Murarka, R. J. Gutmann, A. E. Kaloyerous, and W. A. Lanford, *Thin Solid Films*, **236**, 257 (1993).
2. P. C. Andricacos, C. Uzoh, J. O. Dukovic, J. Horkans, and H. Deligianni, *IBM J. Res. Dev.*, **42**, 567 (1998).
3. R. Rosenberg, D. C. Edelstein, C. K. Hu, and K. P. Rodbell, *Annu. Rev. Mater. Sci.*, **30**, 229 (2000).
4. J. M. Steigerwald, S. P. Murarka, R. J. Gutmann, and D. J. Duquette, *J. Electrochem. Soc.*, **141**, 3512 (1994).
5. M. Fayolle and F. Ronagna, *Microelectron. Eng.*, **37-38**, 135 (1997).
6. V. Nguyen, H. Van Kranenburg, and P. Woerlee, *Microelectron. Eng.*, **50**, 403 (2000).
7. T. H. Tsai and S. C. Yen, *Appl. Surf. Sci.*, **210**, 190 (2003).
8. J. W. Lee, M. C. Kang, and J. J. Kim, *J. Electrochem. Soc.*, **152**, C827 (2005).
9. S. Kondo, N. Sakuma, Y. Homma, and N. Ohashi, *Jpn. J. Appl. Phys., Part 1*, **39**, 6216 (2000).
10. D. Ernur, S. Kondo, D. Shamiryan, and K. Maex, *Microelectron. Eng.*, **64**, 117 (2002).
11. S. Tamilmani, W. Huang, and S. Raghavan, *J. Electrochem. Soc.*, **153**, F53 (2006).
12. E. Paul, F. Kaufmann, V. Brusic, J. Zhang, F. Sun, and R. Vacassy, *J. Electrochem. Soc.*, **152**, G322 (2005).
13. Y. Wang and Y. Zhao, *Appl. Surf. Sci.*, **254**, 1517 (2007).
14. V. R. K. Gorantla, A. Babel, S. Pandija, and S. V. Babu, *Electrochem. Solid-State Lett.*, **8**, G131 (2005).
15. S. Aksu, *J. Electrochem. Soc.*, **152**, G938 (2005).
16. V. R. K. Gorantla, D. Goia, E. Matijevic, and S. V. Babu, *J. Electrochem. Soc.*, **152**, G912 (2005).
17. Y.-F. Wu and T.-H. Tsai, *Microelectron. Eng.*, **84**, 2790 (2007).
18. V. R. K. Gorantla, K. A. Assiongbon, S. V. Babu, and D. Roy, *J. Electrochem. Soc.*, **152**, G404 (2005).
19. M. C. Kang, H.-S. Nam, H. Y. Won, S. Jeong, H. Jeong, and J. J. Kim, *Electrochem. Solid-State Lett.*, **11**, H32 (2008).
20. H. Lee, S. S. Wong, and S. D. Lopatin, *J. Appl. Phys.*, **93**, 3796 (2003).
21. H. P. Feng, J. Y. Lin, M. Y. Cheng, Y. Y. Wang, and C. C. Wan, *J. Electrochem. Soc.*, **155**, H21 (2008).
22. J. Sorooshian, D. DeNardis, L. Charns, Z. Li, F. Shadman, D. Boning, D. Hetherington, and A. Philipossian, *J. Electrochem. Soc.*, **151**, G85 (2004).
23. S. Mudhavarthi, N. Gitis, S. Kuiry, M. Vinogradov, and A. Kumar, *J. Electrochem. Soc.*, **153**, G372 (2006).